

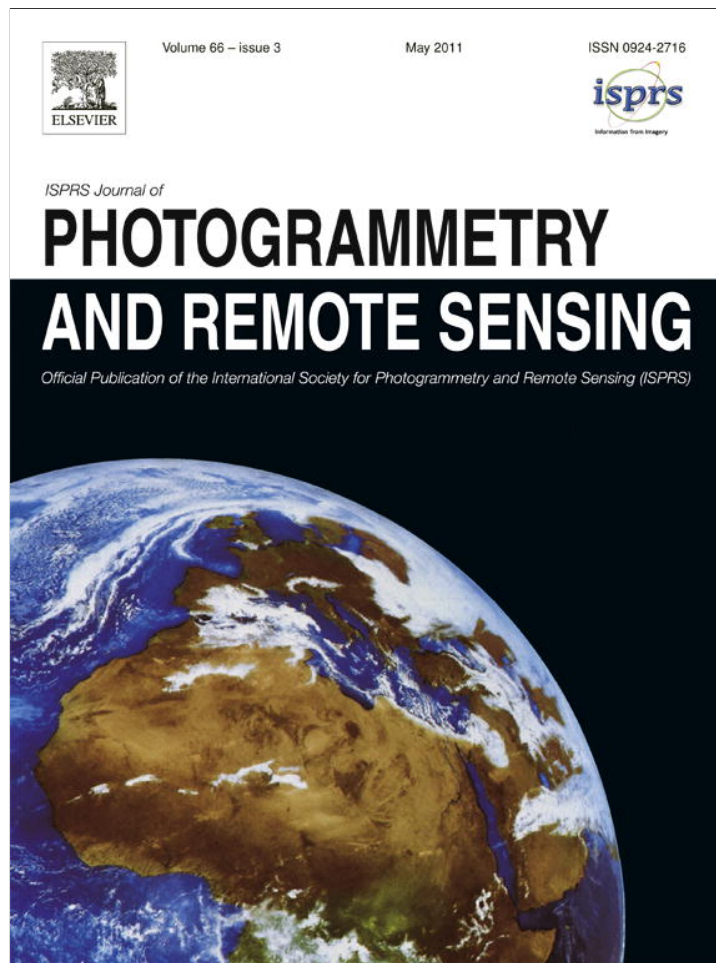


Detection of impervious surface change with multitemporal Landsat images in an urban–rural frontier

Dengsheng Lu, Emilio Moran, Scott Hetrick

In: ISPRS Journal of Photogrammetry and Remote Sensing 66 (2011) 298–306

Provided for non-commercial research and education use.
Not for reproduction, distribution or commercial use.



This article appeared in a journal published by Elsevier. The attached copy is furnished to the author for internal non-commercial research and education use, including for instruction at the authors institution and sharing with colleagues.

Other uses, including reproduction and distribution, or selling or licensing copies, or posting to personal, institutional or third party websites are prohibited.

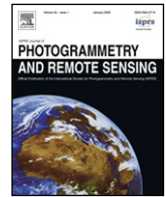
In most cases authors are permitted to post their version of the article (e.g. in Word or Tex form) to their personal website or institutional repository. Authors requiring further information regarding Elsevier's archiving and manuscript policies are encouraged to visit:

<http://www.elsevier.com/copyright>



Contents lists available at ScienceDirect

ISPRS Journal of Photogrammetry and Remote Sensing

journal homepage: www.elsevier.com/locate/isprsjprs

Detection of impervious surface change with multitemporal Landsat images in an urban–rural frontier

Dengsheng Lu*, Emilio Moran, Scott Hetrick

Anthropological Center for Training and Research on Global Environmental Change (ACT), Indiana University, Bloomington, IN, 47405, USA

ARTICLE INFO

Article history:

Received 13 December 2009

Received in revised form

22 October 2010

Accepted 31 October 2010

Available online 26 November 2010

Keywords:

Impervious surfaces

Urban–rural frontier

Landsat

QuickBird

Regression analysis

ABSTRACT

Mapping and monitoring impervious surface dynamic change in a complex urban–rural frontier with medium or coarse spatial resolution images is a challenge due to the mixed pixel problem and the spectral confusion between impervious surfaces and other non-vegetation land covers. This research selected Lucas do Rio Verde County in Mato Grosso State, Brazil as a case study to improve impervious surface estimation performance by the integrated use of Landsat and QuickBird images and to monitor impervious surface change by analyzing the normalized multitemporal Landsat-derived fractional impervious surfaces. This research demonstrates the importance of two-step calibrations. The first step is to calibrate the Landsat-derived fraction impervious surface values through the established regression model based on the QuickBird-derived impervious surface image in 2008. The second step is to conduct the normalization between the calibrated 2008 impervious surface image with other dates of impervious surface images. This research indicates that the per-pixel based method overestimates the impervious surface area in the urban–rural frontier by 50%–60%. In order to accurately estimate impervious surface area, it is necessary to map the fractional impervious surface image and further calibrate the estimates with high spatial resolution images. Also normalization of the multitemporal fractional impervious surface images is needed to reduce the impacts from different environmental conditions, in order to effectively detect the impervious surface dynamic change in a complex urban–rural frontier. The procedure developed in this paper for mapping and monitoring impervious surface area is especially valuable in urban–rural frontiers where multitemporal Landsat images are difficult to be used for accurately extracting impervious surface features based on traditional per-pixel based classification methods as they cannot effectively handle the mixed pixel problem.

© 2010 International Society for Photogrammetry and Remote Sensing, Inc. (ISPRS). Published by Elsevier B.V. All rights reserved.

1. Introduction

Digital change detection in urban environments is a challenge due to the following factors: urban land use/cover changes usually account for a small proportion of the study area and are scattered in different locations; they are often confounded with other changes because of the complexity of impervious surfaces and similar spectral features between impervious surfaces and other non-vegetation land covers; a large number of mixed pixels often result in poor classification accuracy due to the heterogeneous nature of urban environments and the limitation of spatial resolution in the remotely sensed image. Although many change detection techniques, such as principal component analysis, image differencing, and post-classification comparison, can be applied for urban land use and cover change detection (Singh, 1989; Coppin

and Bauer, 1996; Coppin et al., 2004; Lu et al., 2004; Kennedy et al., 2009), the detection results are often poor, especially in urban–rural frontiers. The majority of previous change detection techniques are based on the comparison of spectral responses or classified images at the per-pixel scale. However, per-pixel based methods are problematic in accurately mapping and monitoring urban land use/cover change if medium or coarse spatial resolution images are used (Seto and Liu, 2003; Lu and Weng, 2004). Recent research has indicated that the subpixel-based impervious surface data sets have the potential to detect urban expansion (Yang et al., 2003a; Xian and Crane, 2005; Xian, 2007; Xian et al., 2008).

Urban landscapes can be regarded as a complex combination of buildings, roads, grass, trees, soil, water, and so on. In coarse and medium spatial resolution images such as Landsat Thematic Mapper (TM), mixed pixels have been recognized as a problem in the effective use of remotely sensed data in land use/cover classification and change detection (Fisher, 1997; Cracknell, 1998; Lu and Weng, 2004). As shown in Fig. 1, mixed pixels are common in TM imagery, but this problem almost does not exist in the QuickBird image (0.6 m spatial resolution here). Building shapes,

* Corresponding author. Tel.: +1 812 856 5320; fax: +1 812 855 3000.

E-mail address: dlu@indiana.edu (D. Lu).

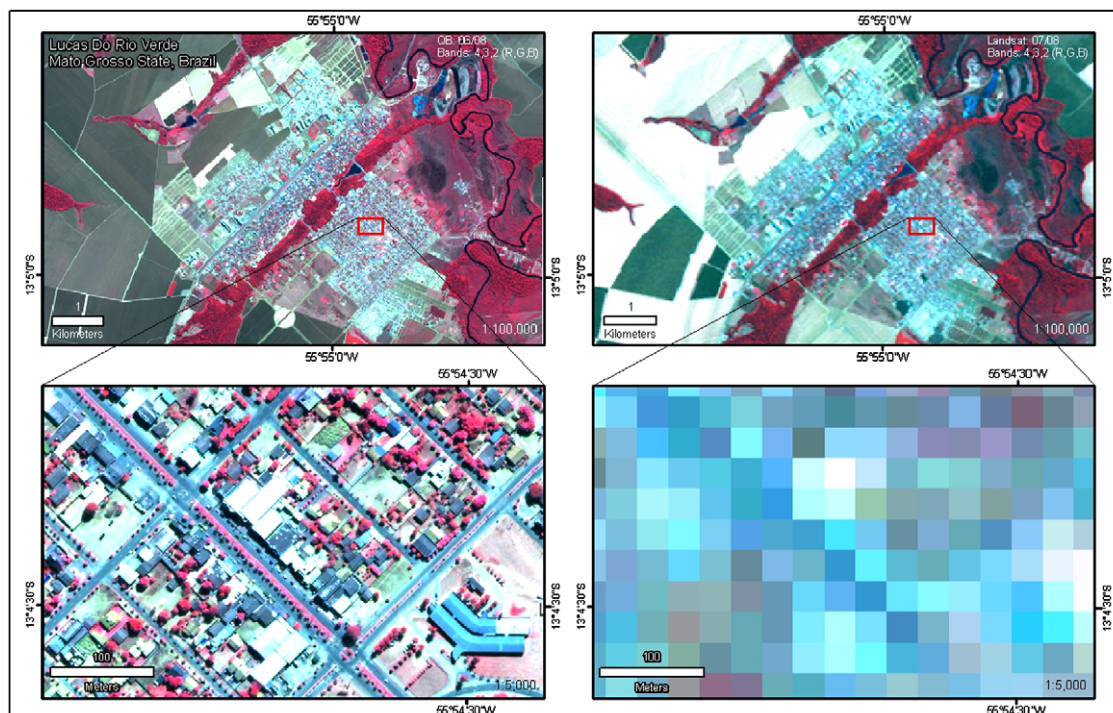


Fig. 1. A comparison of color composites between Landsat TM and QuickBird images (2008), illustrating the mixed pixel problem in relatively coarse spatial resolution images.

roads, and the boundaries between different land covers can be clearly identified on the QuickBird image, but these features cannot be detected in the Landsat TM color composite because of its relatively coarse spatial resolution (i.e., 30 m). This demonstrates the difficulty in urban land use/cover classification or change detection with Landsat TM images. If traditional per-pixel based methods such as the maximum likelihood classifier are used for urban land use/cover classification, urban areas may be significantly overestimated, but rural areas may be significantly underestimated (Lu and Weng, 2004). This situation worsens if multitemporal remote sensing data are used for urban land use/cover change detection, especially in the urban–rural frontiers. It is imperative to develop some new methods that can be used effectively to detect the dynamic change of urban land use/cover at the subpixel level with limited or no training samples for the historical remote sensing data.

Impervious surfaces are generally defined as any anthropogenic materials that water cannot infiltrate and are primarily associated with human activities and habitation through construction of transportation and buildings (Slonecker et al., 2001). Research on impervious surface extraction from remotely sensed data has attracted interest since the 1970s (Slonecker et al., 2001; Brabec et al., 2002; Weng, 2007). Many methods have been developed for mapping impervious surfaces with different spatial resolution images from high spatial resolution such as IKONOS and QuickBird (Mohapatra and Wu, 2008; Lu and Weng, 2009; Wu, 2009), medium spatial resolution such as Landsat TM and Terra ASTER (Deguchi and Sugio, 1994; Slonecker et al., 2001; Hodgson et al., 2003; Wu and Murray, 2003; Yang et al., 2003a,b; Dougherty et al., 2004; Jennings et al., 2004; Wu, 2004; Xian and Crane, 2005; Lu and Weng, 2006a,b; Powell et al., 2008; Wang et al., 2008; Weng et al., 2008; Esch et al., 2009; Hu and Weng, 2009; Weng et al., 2009) and coarse resolution such as DMSP-OLS (Elvidge et al., 2007; Sutton et al., 2009). The main methods include per-pixel image classification (Hodgson et al., 2003; Dougherty et al., 2004; Jennings et al., 2004), subpixel classification (Ji and Jensen, 1999; Phinn et al., 2002; Rashed et al., 2003), neural network (Mohapatra

and Wu, 2008; Wang et al., 2008; Hu and Weng, 2009; Wu, 2009), regression tree model (Yang et al., 2003a,b; Xian and Crane, 2005; Xian, 2008; Xian et al., 2008; Yang et al., 2009), the combination of high-albedo and low-albedo fraction images (Wu and Murray, 2003; Wu, 2004; Lu and Weng, 2006a,b; Weng et al., 2009), and through the established relationship between impervious surfaces and vegetation cover (Gillies et al., 2003; Bauer et al., 2008). However, impervious surface areas are often overestimated or underestimated when medium spatial resolution images are used, depending on the relative proportion of impervious surfaces in a pixel (Wu and Murray, 2003; Lu and Weng, 2006a; Greenfield et al., 2009).

Ridd (1995) assumed that land-cover in urban environments is a linear combination of three components: vegetation, impervious surface, and soil (V–I–S). The V–I–S model provides a guideline for decomposing urban landscapes and a link for these components to remote-sensing spectral characteristics. Several studies have adopted this model as a basis for understanding the urban environment (Madhavan et al., 2001; Rashed et al., 2001; Phinn et al., 2002). Because of the complexity of impervious surfaces in remote sensing spectral signatures and the mixed pixel problem in medium or coarse spatial resolution images (see Fig. 1), subpixel based methods have obtained increasing attention in recent years (Wu and Murray, 2003; Wu, 2004; Lu and Weng, 2006a,b; Weng et al., 2009). These methods are especially valuable for accurately extracting impervious surfaces in the urban–rural landscapes.

Although previous research has explored methods for examining urban expansion based on impervious surface dynamic change (Yang et al., 2003a; Xian, 2007; Powell et al., 2008; Xian et al., 2008), detection of the impervious surface change in a complex urban–rural frontier with medium spatial resolution images remains a challenge. Because increase in impervious surface occurs mainly in the urban–rural frontiers over disperse locations, it is imperative to develop a processing method that can rapidly monitor the impervious surface change in a large area. Therefore, the objectives of this research are (1) to develop a new method to improve impervious surface estimation through the integrated use of Landsat TM

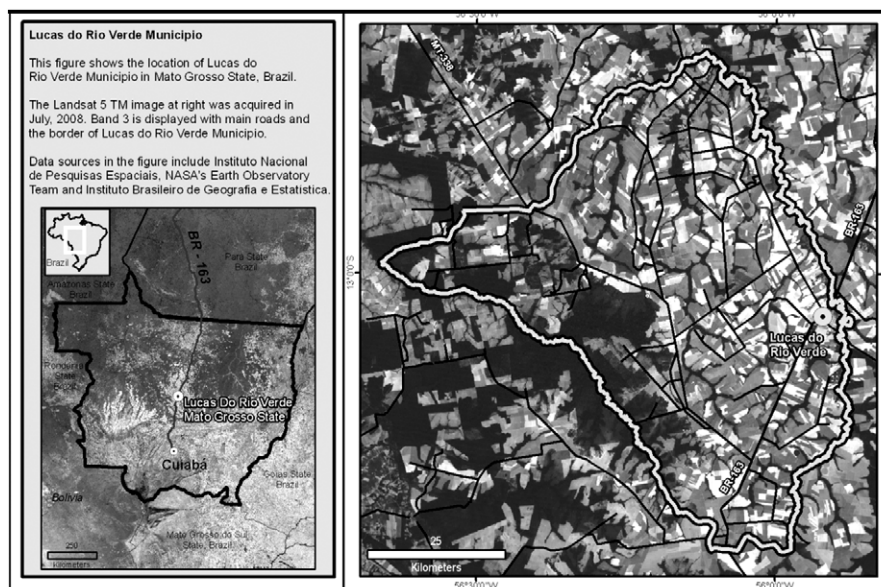


Fig. 2. Study area – Município de Lucas do Rio Verde, Mato Grosso State, Brazil.

Table 1
Landsat and QuickBird images used in research.

Sensor data	Acquisition date	Spectral and spatial resolutions
MSS	July 8 and 9, 1977	Four visible and near infrared bands with 80 m spatial resolution
	June 21, 1984	
	August 9, 1990	
TM	June 6, 1996	Three visible bands (blue, green, and red), one near infrared (NIR) band, and two shortwave infrared (SWIR) bands with 30 m spatial resolution
	September 17, 2002	
	July 17, 2005	
	June 21, 2007	
	May 22, 2008	
ETM	August 10, 1999	The same as TM, but including one panchromatic band with 15 m spatial resolution
QuickBird	April 2, 2007	Three visible bands (blue, green, and red) and one near infrared (NIR) band with 2.4 m, and one panchromatic band with 0.6 m spatial resolution
	June 20, 2008	

and QuickBird images and (2) to examine urban expansion through the analysis of normalized multitemporal impervious surface images.

2. Study area and data sets

2.1. Description of the study area

Lucas do Rio Verde (hereafter called simply Lucas) in Mato Grosso State, Brazil has a small urban extent with a relatively short history, covering a proximate area of 3660 km² with flat terrain (see Fig. 2). It was established in the early 1980s and has experienced a rapid urbanization since then. The study area includes both an urban area, defined in Brazil as a county seat with a population size of approximately 29,000 and rural areas distant from any urban places where the primary activities are agricultural and pastoral activity. The region is connected to Santarém, a river port in the Amazon, and to the heart of the soybean growing area at Cuiabá by the BR-163 highway which runs through the município and its county seat. The economic base of Lucas is large-scale agriculture, including the production of soy, cotton, rice, and corn as well as poultry and swine. The county is at the epicenter of soybean production in Brazil, and it is expected to grow in population three-fold in the next ten years (personal communication with secretariat for planning at Lucas). Annual precipitation is around 2032–2286 mm, mainly starting in September to ending in April. The dry season is between May

and August. The major vegetation includes primary forest, cerrado, and limited areas of plantation and regenerating vegetation. Deforestation was begun in the late 1970s with the construction of the BR-163 highway, especially after the establishment of Lucas County. According to the census data, the population in Lucas was 4332 in 1991, increased to 16,145 in 2000 and to 28,017 in 2007 (<http://www.citypopulation.de/Brazil-MatoGrosso.html>). Because it is, at present, a relatively small town yet has complex urban–rural spatial patterns derived from its highly capitalized agricultural base, large silos and warehouses, and planned urban growth, Lucas is an ideal site for exploring the approaches to map and monitor the impervious surface dynamic change.

2.2. Data sets used in research

Landsat images from 1977 to 2008 and QuickBird images acquired in 2007 and 2008 were used in this research (see Table 1). The quality of time series Landsat images was first visually examined in order to find cloud-free images and those with minimal system-induced errors such as stripping or bad pixels. For all selected Landsat images, radiometric and atmospheric calibration was conducted with the image-based dark-object subtraction method (Lu et al., 2002; Chander et al., 2009). All images were geometrically registered into a UTM (zone 21, south) projection with geometric errors of less than one pixel, so that all images have the same coordinate system. The nearest neighbor resampling technique was used to resample the Landsat

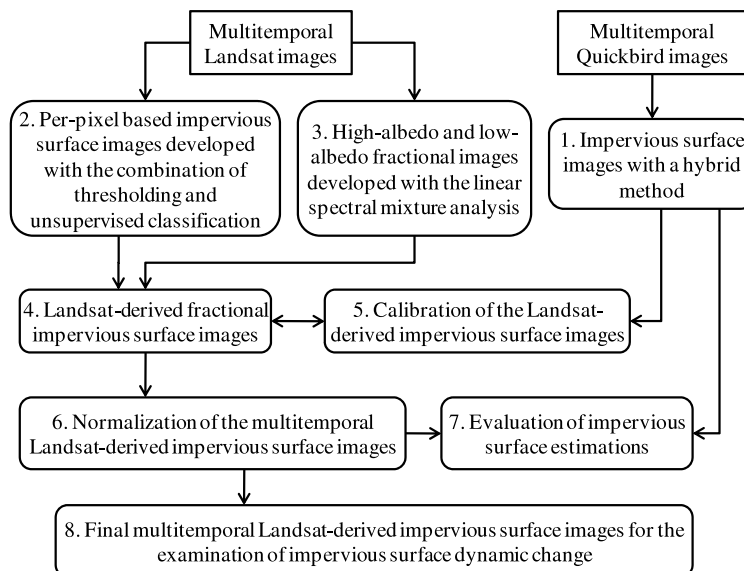


Fig. 3. Strategy of integrating Landsat TM and QuickBird images for mapping impervious surfaces and of monitoring impervious surface dynamic change.

images into a pixel size of 30 m by 30 m during image-to-image registration.

3. Methods

One critical step in this research is to map impervious surface data sets, which is difficult in a complex urban–rural frontier based on Landsat images. In order to improve impervious surface mapping performance, QuickBird imagery is used to calibrate the Landsat-derived impervious surface image. The strategy of mapping and monitoring impervious surface change is illustrated in Fig. 3. The major steps include (1) mapping impervious surfaces with a hybrid method based on QuickBird imagery; (2) extracting per-pixel impervious surface images from Landsat images based on the thresholding of maximum and minimum filtering images and unsupervised classification; (3) mapping fractional images of high-albedo, low-albedo, vegetation, and soil endmembers with the linear spectral mixture analysis; (4) producing fractional impervious surface images by adding high-albedo and low-albedo fraction images while removing non-impervious surface pixels by combining the per-pixel impervious surface images from step 2; (5) establishing a regression model to calibrate the 2008 Landsat-derived impervious surfaces using the 2008 QuickBird-derived impervious surface imagery; (6) normalizing multitemporal Landsat-derived impervious surface images; (7) evaluating impervious surface estimates with the 2007 QuickBird-derived impervious surface imagery; and finally (8) examining impervious surface dynamic change. The following subsections provided detailed descriptions for these steps.

3.1. Mapping impervious surfaces with QuickBird imagery

The QuickBird images were used to develop impervious surface images at a local scale, and the developed impervious surface images were used for establishing a calibration model for modifying the Landsat-derived impervious surface image and for evaluating the results independently. QuickBird imagery has four multispectral bands with 2.4 m spatial resolution and one panchromatic band with 0.6 m spatial resolution. In order to make full use of both the multispectral and panchromatic images, the wavelet merging technique (Lu et al., 2008) was used to merge the QuickBird multispectral bands and panchromatic band into a new multispectral image with 0.6 m spatial resolution. A hybrid method which consisted of thresholding, unsupervised classification, and

manual editing was used to produce the impervious surface image from the fused QuickBird imagery (Lu et al., 2010).

In general, vegetation has significantly different spectral features compared to impervious surfaces in the normalized difference vegetation index (NDVI) image. Clear and deep water bodies have much lower spectral values than impervious surfaces in the near infrared (NIR) wavelength image. Therefore, the vegetation and water pixels can be masked out with selected thresholds on NDVI and NIR images. The major steps for the hybrid approach included: (1) producing the NDVI image from QuickBird red and NIR images and then masking vegetation out with the selected threshold on the NDVI image; and masking water out with the selected thresholds on the NIR image; (2) extracting spectral signatures of the non-vegetation pixels; using an unsupervised classification algorithm to classify the extracted spectral signatures into 50 clusters and then merging the clusters into impervious surfaces and other classes; (3) manually editing the extracted impervious surface image to eliminate the non-impervious surface pixels such as bare soils, shadows, and wetlands which are confused with the impervious surface class due to similar spectral features (Lu et al., 2010).

Although unsupervised classification can separate most impervious surfaces from bare soils and wetlands, some confusion still remains between bare soil and bright impervious surfaces, and among dark impervious surfaces, shadowed impervious surfaces, wetlands or shadows from tree crowns. Therefore, visually examining the extracted impervious surface image is necessary to further refine the impervious surface image quality by eliminating the confused pixels, e.g., bare soils, non-impervious surface shadows, and wetlands. These impervious surface images with spatial resolution of 0.6 m were resampled to 30 m to generate fractional impervious surface images for use as reference data. This method was used to map impervious surface distribution for the 2007 and 2008 QuickBird images. The accuracy assessment based on 450 randomly selected sample plots indicated that overall accuracy of 98% for both 2007 and 2008 QuickBird images was achieved, based on visual interpretation on the QuickBird color composite.

3.2. Developing per-pixel based impervious surfaces from Landsat images

Per-pixel impervious surface mapping is often based on the image classification of spectral signatures (Shaban and Dikshit,

2001; Hodgson et al., 2003; Dougherty et al., 2004; Jennings et al., 2004), but medium or coarse spatial resolution images often generate relatively poor results, especially in a complex urban–rural frontier, because of the spectral confusion between impervious surfaces and other land covers and the mixed pixel problems (Wu and Murray, 2003; Lu and Weng, 2006a,b). This research for mapping per-pixel impervious surfaces was based on the combination of filtering images and unsupervised classification of Landsat spectral signatures. The fact that the red-band images in Landsat TM/ETM+/MSS have high spectral values for impervious surfaces but have low spectral values for vegetation and water/wetland provides a potential to rapidly map impervious surface areas. The minimum and maximum filter with a window size of 3×3 pixels was separately applied to the Landsat red band image. The image differencing between maximum and minimum filtering images was used to highlight linear features (mainly roads) and other impervious surfaces. Examining the differencing image indicated that a threshold of 13 (the value from the differencing image) can be used to extract the impervious surface image. The spectral signature of the initial impervious surface image was then extracted and was further classified into 60 clusters using an unsupervised classification method, to refine the impervious surface image by removing the pixels with non-impervious surfaces. Finally, manual editing of the impervious surface image was conducted to make sure that all impervious surfaces, especially in urban regions, were extracted. The same procedure was applied to all selected Landsat images to generate the per-pixel based time series impervious surface data sets.

3.3. Developing fractional images with linear spectral mixture analysis

As per-pixel methods based on medium or coarse spatial resolution often overestimate or underestimate impervious surface areas, it is important to estimate fractional impervious surface images in order to improve area estimation. Of the many methods for mapping impervious surfaces (Slonecker et al., 2001; Brabec et al., 2002), the linear spectral mixture analysis (LSMA)-based method has proven valuable for extracting fractional impervious surfaces from Landsat images (Wu and Murray, 2003; Lu and Weng, 2006a). LSMA is regarded as a physically based image processing tool. It supports repeatable and accurate extraction of quantitative sub-pixel information (Smith et al., 1990). The LSMA approach assumes that the spectrum measured by a sensor is a linear combination of the spectra of all components (endmembers) within the pixel and that the spectral proportions of the endmembers reflect proportions of the area covered by distinct features on the ground (Adams et al., 1995). A detailed description of LSMA is found in previous literature (e.g. Smith et al., 1990; Lu and Weng, 2004).

From the view of remotely sensed data, the urban landscape can be assumed a combination of four components: high-albedo objects, low-albedo objects, vegetation, and soil (Lu and Weng, 2004, 2006a). Previous research has indicated that the fraction images which are developed with LSMA have physical meaning (Wu and Murray, 2003; Lu and Weng, 2006a). The high-albedo fraction image highlights land covers with high spectral reflectance, such as bright impervious surfaces and dry bare soils; and the low-albedo fraction image highlights the land covers with low spectral reflectance, such as dark impervious surfaces, forested shade, water and wetlands. The soil fraction image highlights soil information, mainly located in agriculture and pasture lands and the vegetation fraction image highlights the forest and plantation information. Impervious surfaces are mainly concentrated in high-albedo and low-albedo fraction images (Lu and Weng, 2006a,b).

In the LSMA approach, the selection of suitable endmembers is a key to successfully extracting fractional images. The minimum

noise fraction transform (MNF) is often used to convert Landsat images into a new data set to support the selection of high quality endmembers. Four endmembers: vegetation, low-albedo, high-albedo, and soil, were identified from the MNF components (Lu and Weng, 2006a). A constrained least squares solution was then used to unmix the Landsat TM/ETM image into four fractional images and one error image. Because MSS has only four bands and the study area had very limited impervious surfaces in 1977, three endmembers (i.e., high-albedo, low-albedo and vegetation) were used.

3.4. Developing fractional impervious surface images through the combination of fractional images and per-pixel impervious surface images

One critical step in mapping impervious surfaces is the removal of impervious surface free pixels. By combining per-pixel impervious surfaces with high-albedo and low-albedo fraction images, a fractional impervious surface image was generated with the following rules: if the pixel is an impervious surface in the per-pixel based impervious surface image, then that pixel is extracted from the sum of high-albedo and low-albedo fraction images; otherwise, zero is assigned to the pixel. This procedure was used separately to map fractional impervious surface images from the multitemporal Landsat images.

3.5. Refining impervious surface areas by the integrated use of Landsat- and QuickBird-derived impervious surface images

Previous research has indicated that impervious surface areas developed from Landsat TM images are often overestimated or underestimated, depending on the proportion of impervious surfaces in a pixel (Wu and Murray, 2003; Lu and Weng, 2006a). One method which can be used to calibrate this bias is to develop a regression model to calibrate the TM-derived impervious surface images. In this research, the overlap area between the 2008 QuickBird-derived and the corresponding Landsat-derived impervious surface images were selected and used for sample collection based on the selection of one pixel for every five on the overlapped images. Because many pixels were non-impervious surfaces, they had zero values. After removal of all samples with zero values, 1512 samples were used to develop the calibration model. A scatterplot-based method was used to examine the relationship between both the 2008 Landsat-derived and QuickBird-derived impervious surface images. A regression model was developed to conduct the calibration.

3.6. Refining the multitemporal impervious surface images by image-to-image normalization

The mapping of impervious surface areas from time series remote sensing images can often be affected by different environmental conditions, such as soil moisture, atmospheric conditions, and vegetation phenology (Wu and Yuan, 2008; Hu and Weng, 2009). It is therefore necessary to calibrate the bias caused by these different conditions. It can be assumed that the same invariant locations in different dates of Landsat images should have the same fraction impervious surface areas in a pixel. Thus, a calibration model can be developed to calibrate the multitemporal impervious surface images. All the Landsat-derived fractional impervious surface images were stacked into one file. Pseudo-invariant objects, i.e., unchanged impervious surface objects from the time series fractional impervious surface images were selected. A total of 24 sample points were selected along the major highway and urban areas, with the assumption that the unchanged impervious surfaces have the same fraction value in a pixel.

A regression model corresponding to each pair of images was developed based on the relationship between the reference data from the calibrated 2008 fractional impervious surface image and subject images from other dates of Landsat-derived fractional impervious surface images. The regression models were then used to calibrate the extracted impervious surface images in order to reduce the impervious surface estimation bias caused by external factors such as different vegetation phenology and atmospheric conditions.

3.7. Evaluating the extracted fractional impervious surface images

Evaluation of impervious surface estimates can be challenging due to the difficulty in obtaining reference data, especially for historical data sets. High spatial resolution images such as aerial photographs and QuickBird images are often used to collect reference data. In this research, a 2007 QuickBird-derived impervious surface image was used to evaluate the 2007 Landsat TM-derived fractional impervious surface image after image normalization. The impervious surface image developed from the 2007 QuickBird image with 0.6 m spatial resolution was resampled to 30 m to produce a fractional impervious surface image. In order to reduce the geometric error between the QuickBird- and TM-derived impervious surface images, a window size of 3×3 pixels was used to select samples, based on the overlap area on both 2007 QuickBird- and TM-derived impervious surface images. Scatterplot analysis, correlation analysis, and root mean square error (RMSE) were used to examine the quality of the TM-derived fractional impervious surface image.

3.8. Examining the impervious surface dynamic change

In the urban–rural frontier, impervious surface increase is mainly due to the construction of individual buildings and roads. Because the areas of these objects are often smaller than the pixel size of Landsat images, geometric accuracies between the multitemporal images become critical for successful detection of impervious surface change. In this study area, due to the geometric errors between multitemporal Landsat images (less than one pixel) and small width of roads (usually smaller than the pixel size of the Landsat TM/ETM images), it is hard to spatially examine the impervious surface change with the pixel-by-pixel comparison of multitemporal impervious surface images. Therefore, a total impervious surface area for each date was calculated. The scatterplots showing relationships between total impervious surface areas and dates were developed to examine the impervious surface change trends.

4. Results and discussions

4.1. Calibration of the Landsat-derived fractional impervious surfaces with the QuickBird-derived impervious surface image

In theory, if the impervious surfaces are accurately estimated from both TM and QuickBird images, the scatterplot between both variables should show a very good linear relationship. As shown in Fig. 4, the impervious surface image developed in this research demonstrates a reasonably good result, although overestimation occurred when the impervious surfaces accounted for a relatively small proportion in a pixel and underestimation occurred when the impervious surfaces accounted for a large proportion in a pixel. This trend is similar to other previous research (Wu and Murray, 2003; Lu and Weng, 2006a,b; Greenfield et al., 2009). Overall, a good linear relationship exists between the fractional impervious surface images developed independently from 2008 Landsat TM and QuickBird images. Based on the samples from QuickBird- and

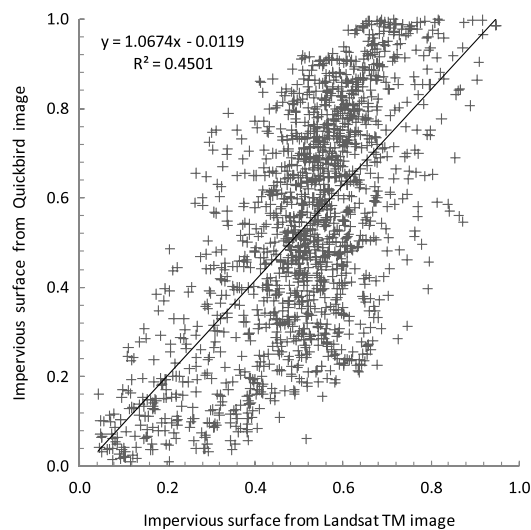


Fig. 4. Relationship of impervious surface values from Landsat TM and QuickBird images.

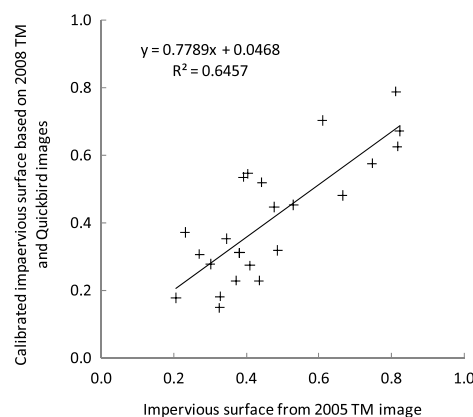


Fig. 5. Relationship of the impervious surface values from different dates of Landsat images.

Landsat-derived impervious surface images, a linear regression model is established as follows:

$$y = 1.0674x - 0.0119, \quad (1)$$

where x is the fractional impervious surface values from 2008 Landsat TM image, and y is the calibrated fraction impervious surface values from the QuickBird image. The coefficient of determination (R^2) is 0.45 for this regression model. This equation was used to calibrate the entire 2008 Landsat TM-derived fractional impervious surface image.

4.2. Normalization of the multitemporal Landsat-derived impervious surface images

Image-to-image normalization is valuable in reducing the impacts caused by different environmental conditions on the impervious surface estimation performance based on multitemporal remotely sensed data (Wu and Yuan, 2008; Hu and Weng, 2009). As an example, Fig. 5 demonstrates a very good linear relationship between the calibrated 2008 TM-derived impervious surface image and 2005 TM-derived impervious surface image. Similar relationships exist for other dates of impervious surface images, as summarized in Table 2. In this research, the 2008 calibrated impervious surface image was used as a reference image, and other dates

Table 2
Regression equations for the normalization of the multitemporal Landsat-derived fractional impervious surface images.

Year	Regression equation	R^2
2007	$y = 0.8148x + 0.1552$	0.70
2005	$y = 0.7789x + 0.0468$	0.65
2002	$y = 0.5354x + 0.2473$	0.62
1999	$y = 0.6305x + 0.2061$	0.65
1996	$y = 0.7093x + 0.1862$	0.61
1990	$y = 0.6688x + 0.1535$	0.60
1984	$y = 0.6253x + 0.0952$	0.76
1977	$y = 0.5353x + 0.0991$	0.47

Note: y is the calibrated fractional impervious surface, and x is the fractional impervious surface before calibration.

of Landsat-derived impervious surface images were used as subject images respectively. The R^2 values for all Landsat-derived impervious surface images were greater than 0.6, except for the MSS image. The good linear relationships indicate that linear regression models can be used to calibrate fractional impervious surface images, thus, improving the performance of impervious surface estimation.

The relatively small R^2 value for the regression model based on the MSS in 1977 may be caused by the following problems: the coarse spatial and spectral resolutions in MSS (80 m, 4 bands) compared with TM/ETM (30 m, 6 bands) make it difficult to accurately map subpixel impervious surfaces based on spectral mixture analysis; the very limited impervious surface areas in 1977 make it difficult in collecting sufficient sample plots for image-to-image normalization, and the geometric correction errors between MSS and other TM images produce location errors during the sample data collection. Another problem is that the assumption of the same invariant locations between 1977 and 2008 may be not true due to the rapid land use/cover change and the different spatial resolution between MSS and TM images.

4.3. Evaluation of the 2007 Landsat-derived impervious surface image with the 2007 QuickBird-derived impervious surface image

A good agreement between the TM-derived impervious surface result and corresponding 2007 QuickBird-derived result was obtained (Fig. 6). The correlation coefficient between them is 0.89 with a RMSE of 0.128. This error is acceptable for such a complex urban–rural frontier. The high correlation coefficient and relatively low RMSE indicate that the 2007 TM-derived impervious surface image is reliable, and also implies that the method developed in this research for estimating fractional impervious surface areas is feasible.

4.4. Analysis of dynamic change in impervious surfaces

The impervious surface expansion from 1977 to 2008 is easily perceived. As part of the study area illustrated in Fig. 7, the spatial distribution of the impervious surface areas expanded rapidly, mainly taking place as urban extent and roads expanded. Overall, impervious surface areas increased at an exponential rate, as shown in Fig. 8, especially the expansion rate was increased after the year 2000. Comparing the increasing rates between per-pixel based impervious surface areas and the fractional impervious surface areas, the impervious surface change trends are similar. However, per-pixel based impervious surface areas can be overestimated by 50%–60% when compared with fractional impervious surface areas, indicating the importance of subpixel based estimation method in the urban–rural areas where impervious surface areas account for very small proportion in the study area. The results illustrated in Fig. 8 demonstrate

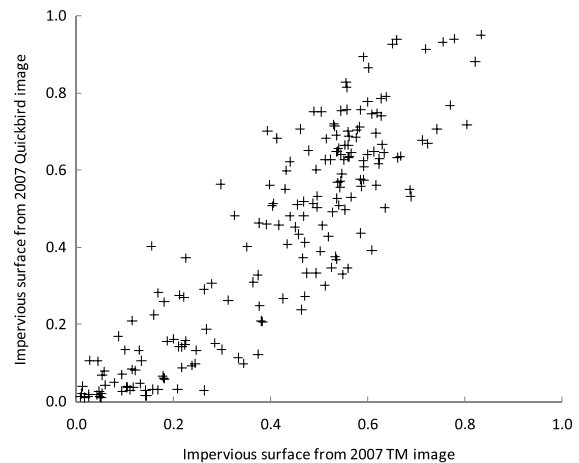


Fig. 6. Accuracy assessment based on QuickBird image in 2007.

importance of the two-step calibration method in improving impervious surface area estimation, especially in urban–rural frontiers, without implementing image classification for historical Landsat images, which are often difficult due to lack of training sample data.

5. Summary

Complex impervious surfaces in the urban landscape and mixed pixels in medium and coarse spatial resolution images make mapping and monitoring of impervious surface change a challenge. Traditional per-pixel based image classification methods cannot effectively handle the mixed pixel problem and subpixel based methods cannot effectively separate the pixels of impervious surfaces from other land covers, thus, underestimation or overestimation of impervious surface areas are common, depending on the proportion of impervious surface in a pixel. The method developed in this paper, which is based on a combination of per-pixel based impervious surface mapping with filtering and unsupervised classification and subpixel based method with LSMA, can effectively map impervious surface distribution with Landsat images. The calibration with QuickBird-derived results can further reduce the bias caused by mixed pixel problems and improve impervious surface mapping performance. The normalization of multitemporal impervious surface images can reduce the bias caused by different environmental conditions in the multitemporal Landsat images, and thus improve the quality of time series impervious surface data sets. Therefore, the use of multitemporal fractional impervious surface images provides a new method for the examination of urban expansion, especially in a complex urban–rural frontier where impervious surfaces only account for a small proportion of the study area. One advantage of the method is that the impervious surface area estimation can be considerably improved when compared with per-pixel based results. Another advantage is that the change detection in a complex urban–rural frontier becomes feasible by the use of multitemporal impervious surface images without the use of training samples for historical remote sensing data, which is often difficult to acquire.

Acknowledgements

The authors wish to thank the National Institute of Child Health and Human Development at NIH (grant # R01 HD035811) for the support of this research, addressing population–and–environment reciprocal interactions in several regions of the Brazilian Amazon.

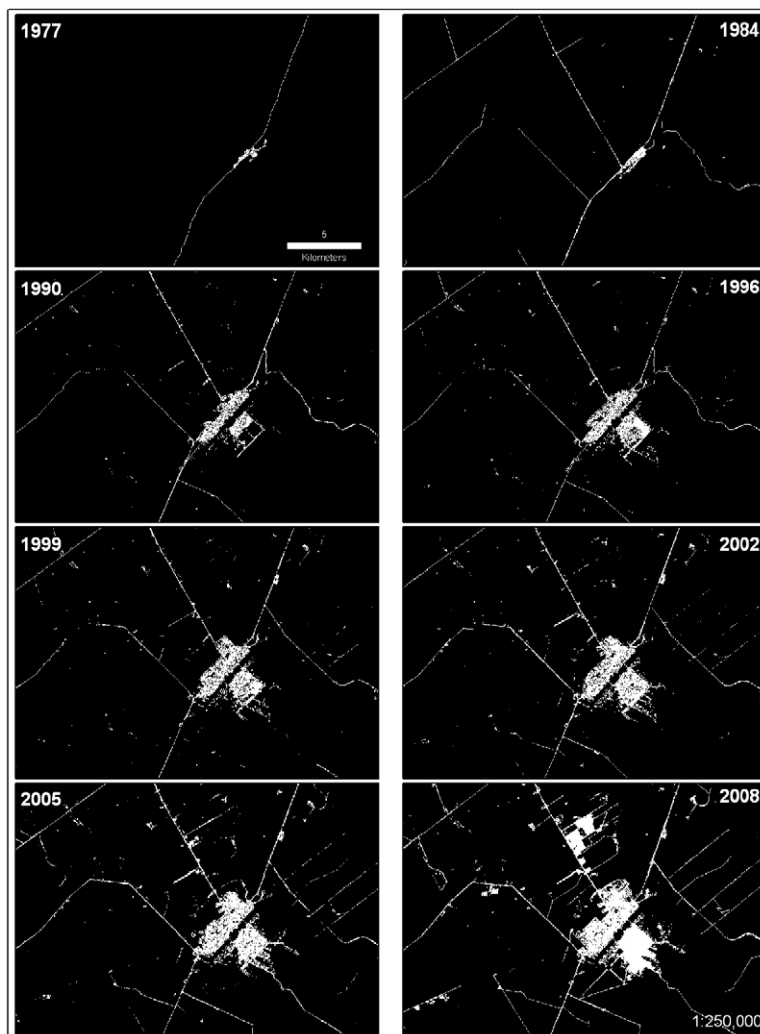


Fig. 7. Impervious surface change from 1977 to 2008, illustrating part of the study area in the município of Lucas, Mato Grosso, Brazil (for the sake of clear display of impervious surface change, per-pixel based impervious surface images were used in this figure).

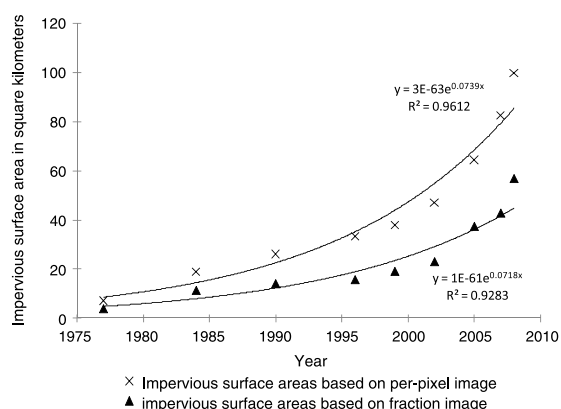


Fig. 8. The impervious surface dynamic change trends between 1977 and 2008.

Any errors are solely the responsibility of the authors and not of the funding agencies.

References

Adams, J.B., Sabol, D.E., Kapos, V., Filho, R.A., Roberts, D.A., Smith, M.O., Gillespie, A.R., 1995. Classification of multispectral images based on fractions of endmembers: application to land cover change in the Brazilian Amazon. *Remote Sensing of Environment* 52 (2), 137–154.

Bauer, M.E., Loffelholz, B.C., Wilson, B., 2008. Estimating and mapping impervious surface area by regression analysis of Landsat imagery. In: Weng, Q. (Ed.), *Remote Sensing of Impervious Surfaces*. Taylor & Francis Group, LLC, Boca Raton, FL, pp. 3–19.

Brabec, E., Schulte, S., Richards, P.L., 2002. Impervious surface and water quality: a review of current literature and its implications for watershed planning. *Journal of Planning Literature* 16 (4), 499–514.

Chander, G., Markham, B.L., Helder, D.L., 2009. Summary of current radiometric calibration coefficients for Landsat MSS, TM, ETM+, and EO-1 ALI sensors. *Remote Sensing of Environment* 113 (5), 893–903.

Coppin, P.R., Bauer, M.E., 1996. Digital change detection in forest ecosystems with remote sensing imagery. *Remote Sensing Reviews* 13 (3), 207–234.

Coppin, P., Jonckheere, I., Nackaerts, K., Muys, B., Lambin, E., 2004. Digital change detection methods in ecosystem monitoring: a review. *International Journal of Remote Sensing* 25 (9), 1565–1596.

Cracknell, A.P., 1998. Synergy in remote sensing – what's in a pixel? *International Journal of Remote Sensing* 19 (11), 2025–2047.

Deguchi, C., Sugio, S., 1994. Estimations for the percentage of impervious area by the use of satellite remote sensing imagery. *Journal of Soil and Water Conservation* 29 (1–2), 135–144.

Dougherty, M., Dymond, R.L., Goetz, S.J., Jantz, C.A., Goulet, N., 2004. Evaluation of impervious surface estimates in a rapidly urbanizing watershed. *Photogrammetric Engineering and Remote Sensing* 70 (11), 1275–1284.

Elvidge, C.D., Tuttle, B.T., Sutton, P.C., Baugh, K.E., Howard, A.T., Milesi, C., Bhaduri, B., Nemani, R., 2007. Global distribution and density of constructed impervious surfaces. *Sensors* 7 (9), 1962–1979.

Esch, T., Himmler, V., Schorcht, G., Thiel, M., Wehrmann, T., Bachofer, F., Conrad, C., Schmidt, M., Dech, S., 2009. Large-area assessment of impervious surface based on integrated analysis of single-date Landsat-7 images and geospatial vector data. *Remote Sensing of Environment* 113 (8), 1678–1690.

Fisher, P., 1997. The pixel: a snare and a delusion. *International Journal of Remote Sensing* 18 (3), 679–685.

- Gillies, R.R., Box, J.B., Symanzik, J., Rodemaker, E.J., 2003. Effects of urbanization on the aquatic fauna of the Line Creek watershed, Atlanta – a satellite perspective. *Remote Sensing of Environment* 86 (3), 411–422.
- Greenfield, E.J., Nowak, D.J., Walton, J.T., 2009. Assessment of 2001 NLCD percent tree and impervious cover estimates. *Photogrammetric Engineering & Remote Sensing* 75 (11), 1279–1286.
- Hodgson, M.E., Jensen, J.R., Tullis, J.A., Riordan, K.D., Archer, C.M., 2003. Synergistic use of Lidar and color aerial photography for mapping urban parcel imperviousness. *Photogrammetric Engineering & Remote Sensing* 69 (9), 973–980.
- Hu, X., Weng, Q., 2009. Estimating impervious surfaces from medium spatial resolution imagery using the self-organizing map and multi-layer perceptron neural networks. *Remote Sensing of Environment* 113 (10), 2089–2102.
- Jennings, D.B., Jarnagin, S.T., Ebert, C.W., 2004. A modeling approach for estimating watershed impervious surface area from national land cover data 92. *Photogrammetric Engineering & Remote Sensing* 70 (11), 1295–1307.
- Ji, M., Jensen, J.R., 1999. Effectiveness of subpixel analysis in detecting and quantifying urban imperviousness from Landsat Thematic Mapper. *Geocarto International* 14 (4), 31–39.
- Kennedy, R.E., Townsend, P.A., Gross, J.E., Cohen, W.B., Bolstad, P., Wang, Y.Q., Adams, P., 2009. Remote sensing change detection tools for natural resource managers: understanding concepts and tradeoffs in the design of landscape monitoring projects. *Remote Sensing of Environment* 113 (7), 1382–1396.
- Lu, D., Mausel, P., Brondizio, E., Moran, E., 2002. Assessment of atmospheric correction methods for Landsat TM data applicable to Amazon basin LBA research. *International Journal of Remote Sensing* 23 (13), 2651–2671.
- Lu, D., Mausel, P., Brondizio, E., Moran, E., 2004. Change detection techniques. *International Journal of Remote Sensing* 25 (12), 2365–2407.
- Lu, D., Weng, Q., 2004. Spectral mixture analysis of the urban landscapes in Indianapolis with Landsat ETM+ imagery. *Photogrammetric Engineering & Remote Sensing* 70 (9), 1053–1062.
- Lu, D., Weng, Q., 2006a. Use of impervious surface in urban land use classification. *Remote Sensing of Environment* 102 (1–2), 146–160.
- Lu, D., Weng, Q., 2006b. Spectral mixture analysis of ASTER images for examining the relationship between urban thermal features and biophysical descriptors in Indianapolis, United States. *Remote Sensing of Environment* 104 (2), 157–167.
- Lu, D., Battistella, M., Moran, E., de Miranda, E.E., 2008. A comparative study of Landsat TM and SPOT HRG images for vegetation classification in the Brazilian Amazon. *Photogrammetric Engineering & Remote Sensing* 74 (3), 311–321.
- Lu, D., Weng, Q., 2009. Extraction of urban impervious surface from an IKONOS image. *International Journal of Remote Sensing* 30 (5), 1297–1311.
- Lu, D., Hetrick, S., Moran, E., 2010. Impervious surface mapping with QuickBird imagery. *International Journal of Remote Sensing*. doi:10.1080/01431161003698393.
- Madhavan, B.B., Kubo, S., Kurisaki, N., Sivakumar, T.V.L.N., 2001. Appraising the anatomy and spatial growth of the Bangkok Metropolitan area using a vegetation-impervious-soil model through remote sensing. *International Journal of Remote Sensing* 22 (5), 789–806.
- Mohapatra, R.P., Wu, C., 2008. Subpixel imperviousness estimation with IKONOS imagery: an artificial neural network approach. In: Weng, Q. (Ed.), *Remote Sensing of Impervious Surfaces*. Taylor & Francis Group, LLC, Boca Raton, FL, pp. 21–37.
- Phinn, S., Stanford, M., Scarth, P., Murray, A.T., Shyy, P.T., 2002. Monitoring the composition of urban environments based on the vegetation-impervious surface-soil (VIS) model by subpixel analysis techniques. *International Journal of Remote Sensing* 23 (20), 4131–4153.
- Powell, S.L., Cohen, W.B., Yang, Z., Pierce, J.D., Alberti, M., 2008. Quantification of impervious surface in the Snohomish water resources inventory area of western Washington from 1972–2006. *Remote Sensing of Environment* 112 (4), 1895–1908.
- Rashed, T., Weeks, J.R., Gadalla, M.S., Hill, A.G., 2001. Revealing the anatomy of cities through spectral mixture analysis of multispectral satellite imagery: a case study of the Greater Cairo region. *Egypt. Geocarto International* 16 (4), 7–18.
- Rashed, T., Weeks, J.R., Roberts, D., Rogan, J., Powell, R., 2003. Measuring the physical composition of urban morphology using multiple endmember spectral mixture models. *Photogrammetric Engineering & Remote Sensing* 69 (9), 1011–1020.
- Ridd, M.K., 1995. Exploring a V–S (Vegetation–Impervious Surface–Soil) model for urban ecosystem analysis through remote sensing: comparative anatomy for cities. *International Journal of Remote Sensing* 16 (12), 2165–2185.
- Seto, K.C., Liu, W., 2003. Comparing ARTMAP neural network with the maximum-likelihood classifier for detecting urban change. *Photogrammetric Engineering and Remote Sensing* 69 (9), 981–990.
- Shaban, M.A., Dikshit, O., 2001. Improvement of classification in urban areas by the use of textural features: the case study of Lucknow city, Uttar Pradesh. *International Journal of Remote Sensing* 22 (4), 565–593.
- Singh, A., 1989. Digital change detection techniques using remotely sensed data. *International Journal of Remote Sensing* 10 (6), 989–1003.
- Slonecker, E.T., Jennings, D., Garofalo, D., 2001. Remote sensing of impervious surface: a review. *Remote Sensing Reviews* 20 (3), 227–255.
- Smith, M.O., Ustin, S.L., Adams, J.B., Gillespie, A.R., 1990. Vegetation in Deserts: I. A regional measure of abundance from multispectral images. *Remote Sensing of Environment* 31 (1), 1–26.
- Sutton, P.C., Anderson, S.A., Elvidge, C.D., Tuttle, B.T., Ghosh, T., 2009. Paving the planet: impervious surface as proxy measure of the human ecological footprint. *Progress in Physical Geography* 33 (4), 510–527.
- Wang, Y., Zhou, Y., Zhang, X., 2008. The SPLIT and MASC models for extraction of impervious surface areas from multiple remote sensing data. In: Weng, Q. (Ed.), *Remote Sensing of Impervious Surfaces*. Taylor & Francis Group, LLC, Boca Raton, FL, pp. 77–92.
- Weng, Q. (Ed.), 2007. *Remote Sensing of Impervious Surfaces*. Taylor & Francis Group, LLC, Boca Raton, FL, 454 p.
- Weng, Q., Hu, X., Lu, D., 2008. Extracting impervious surface from medium spatial resolution multispectral and hyperspectral imagery: a comparison. *International Journal of Remote Sensing* 29 (11), 3209–3232.
- Weng, Q., Hu, X., Liu, H., 2009. Estimating impervious surfaces using linear spectral mixture analysis with multitemporal ASTER images. *International Journal of Remote Sensing* 30 (18), 4807–4830.
- Wu, C., Murray, A.T., 2003. Estimating impervious surface distribution by spectral mixture analysis. *Remote Sensing of Environment* 84 (4), 493–505.
- Wu, C., 2004. Normalized spectral mixture analysis for monitoring urban composition using ETM+ imagery. *Remote Sensing of Environment* 93 (4), 480–492.
- Wu, C., Yuan, F., 2008. Seasonal sensitivity analysis of impervious surface estimation with satellite imagery. *Photogrammetric Engineering & Remote Sensing* 73 (12), 1393–1402.
- Wu, C., 2009. Quantifying high-resolution impervious surfaces using spectral mixture analysis. *International Journal of Remote Sensing* 30 (11), 2915–2932.
- Xian, G., Crane, M., 2005. Assessments of urban growth in the Tampa Bay watershed using remote sensing data. *Remote Sensing of Environment* 97 (2), 203–215.
- Xian, G., 2007. Assessing urban growth with subpixel impervious surface coverage. In: Weng, Q., Quattrochi, D.A. (Eds.), *Urban Remote Sensing*. Taylor & Francis Group, LLC, Boca Raton, FL, pp. 179–200.
- Xian, G., 2008. Mapping impervious surfaces using classification and regression tree algorithm. In: Weng, Q. (Ed.), *Remote Sensing of Impervious Surfaces*. Taylor & Francis Group, LLC, Boca Raton, FL, pp. 39–58.
- Xian, G., Crane, M.P., McMahon, C., 2008. Quantifying multitemporal urban development characteristics in Las Vegas from Landsat and Aster data. *Photogrammetric Engineering & Remote Sensing* 74 (4), 473–481.
- Yang, L., Xian, G., Klaver, J.M., Deal, B., 2003a. Urban land-cover change detection through sub-pixel imperviousness mapping using remotely sensed data. *Photogrammetric Engineering & Remote Sensing* 69 (9), 1003–1010.
- Yang, L., Huang, C., Homer, C., Wylie, B., Coan, M., 2003b. An approach for mapping large-area impervious surface: synergistic use of Landsat 7 ETM+ and high spatial resolution imagery. *Canadian Journal of Remote Sensing* 29 (2), 230–240.
- Yang, L., Jiang, L., Lin, H., Liao, M., 2009. Quantifying sub-pixel urban impervious surface through fusion of optical and InSAR imagery. *GIScience and Remote Sensing* 46 (2), 161–171.

2010

No. 10-03

Lu, D., S. Hetrick, and E. Moran 2010. Land Cover Classification in a Complex Urban-rural Landscape with QuickBird Imagery. *Photogrammetric Engineering & Remote Sensing* 76(10):1159-1168.

No. 10-04

Lu, D., E. Moran, S. Hetrick and G. Li. In Press. Mapping Impervious Surface Distribution with the Integration of Landsat TM and Quickbird Images in a Complex Urban-rural Frontier in Brazil. Chapter 16.

No. 10-05

Lu, D., S. Hetrick, and E. Moran. In Press. Impervious Surface Mapping with Quickbird Imagery. *International Journal of Remote Sensing*.

No. 10-06

Mattos, L. and A. Cau. In Press. The Clean Development Mechanism and Agroforestry Activities in the Brazilian Amazon.

No. 10-09

Lu, D., E. Moran, and S. Hetrick. In Press. Detection of Impervious Surface Change with Multitemporal Remote Sensing Data in an Urban-rural Frontier.

No. 10-10

D. Lu, S. Hetrick, E. Moran, and G. Li. In Press. Detection of Urban Expansion with Multitemporal Quickbird Images. *International Journal of Remote Sensing*.

No. 10-11

Muehlenbein, M.P., J.L. Hirschtick, J.Z. Bonner, and A.M. Swartz. 2010. Toward quantifying the usage costs of human immunity: Altered metabolic rates and hormone levels during acute immune activation in men. *American Journal of Human Biology* 22: 546-556.

No. 10-12

Muehlenbein, M.P., L.A. Martinez, A.A. Lemke, L. Ambu, S. Nathan, S. Alsito, and R. Sakong. 2010. Unhealthy travelers present challenges to sustainable primate ecotourism. *Travel Medicine and Infectious Disease* 8: 169-175.

No. 10-13

Tucker, C.M. 2010. Private Goods and Common Property: Pottery Production in a Honduran Lenca Community. *Human Organization* 69(1): 43-53.

No. 10-14

Tucker, C.M., H. Eakin, and E.J. Castellanos. 2010. Perceptions of risk and adaptation: Coffee producers, market shocks, and extreme weather in Central America and Mexico. *Global Environmental Change* 20: 23-32.

No. 10-15

Lu, D., S. Hetrick, E. Moran, and G. Li. 2010. Detection of Urban Expansion in an Urban-rural Landscape with Multitemporal QuickBird Images. *Journal of Applied Remote Sensing* 4(041880): 1-17.

No. 10-16

Mattos, L., E. Brondizio, A. Romeiro, and R. Orair. 2010. Agricultura de pequena escala e suas implicações na transição agroecológica na Amazônia Brasileira. *Amazônica* 2(2): 220-248.